Journal of Computer and Communications, 2020, 8, 1-6
https://www.scirp.org/journal/jcc
ISSN Online: 2327-5227
ISSN Print: 2327-5219

Axial Micro-Strain Sensor Based on FM-FBG via Dual-Mode ML-FMF in Sensor Networks

Xiao Liang[1*], Zhaoxin Geng[1], Jingcong Li[1], Pengyu Zhang[2], Wenqiang Liu[3]

[1]School of Information Engineering, Minzu University of China, Beijing, China
[2]Changchun Electrical Services Section of China Railway Shenyang Group Co., Ltd., Changchun, China
[3]CRRC QISHUYAN Institute Co., Ltd., Changzhou, China
Email: *bjtulxlx@sina.com

How to cite this paper: Liang, X., Geng, Z.X., Li, J.C., Zhang, P.Y. and Liu, W.Q. (2020) Axial Micro-Strain Sensor Based on FM-FBG via Dual-Mode ML-FMF in Sensor Networks. *Journal of Computer and Communications*, **8**, 1-6.
https://doi.org/10.4236/jcc.2020.810001

Received: May 25, 2020
Accepted: October 19, 2020
Published: October 22, 2020

Abstract

An in-fiber axial micro-strain sensor based on a Few Mode Fiber Bragg Grating (FM-FBG) is proposed and experimentally characterized. This FM-FBG is in inscribed in a multi-layer few-mode fiber (ML-FMF), and could acquire the change of the axial strain along fibers, which depends on the transmission dips. On account of the distinct dual-mode property, a good stability of this sensor is realized. The two transmission dips could have the different sensing behaviors. Both the propagation characteristics and operation principle of such a sensor are demonstrated in detail. High sensitivity of the FM-FBG, ~4 pm/με and ~4.5 pm/με within the range of 0 με - 1456 με, is experimentally achieved. FM-FBGs could be easily scattered along one fiber. So this sensor may have a great potential of being used in sensor networks.

Keywords

Micro-Strain Sensor, ML-FMF, Dual-Mode Fiber, FM-FBG, Sensor Network

1. Introduction

In recent years, in-fiber strain sensors based on Fiber Bragg gratings (FBGs) have been paid more attention in monitoring the axial micro-strain, and their unique advantages show a high degree of accuracy, fast response, high immunity to electromagnetic interference, long-range operation capability, low cost and easy to manufacture [1]. The sensing principle of the FBG sensor is based on the demodulation of the reflection spectra in response to strain [2] [3], temperature [4] [5], surrounding refractive indexes (SRI), pressure [6] [7], acceleration [8], and tilt angle [9]. To date, a great many of sensor designs based on few mode FBGs (FM-FBG) have been reported. The FM-FBG has unique spectrum characteristics, which has more flexibility in a composite detection system. It has already been widely utilized in FBG sensors, application scenarios ranging from strain, temperature, solution concentration and refractive index [10]-[15]. Compared with the traditional temperature sensing scheme, the strain FBG sensor based on a dual mode multi-layer few-mode fiber (ML-FMF) in this paper takes into account the well characteristics of simple structure and well sensitivity.

In this work, we demonstrate an axial micro-strain sensor on the basis of an in-fiber FM-FBG inscribed in the ML-FMF. The micro-strain is vital factors affecting the performance of fiber sensors. The sensing property of transmission dips in the ML-FMF based FM-FBGs will perform varying degrees of deviation with axial strain. According to the results of sensing experiments, the strain causes a change in wavelength shifted. The propagation characteristic and operation principle of this advanced sensor is introduced meticulously.

2. Axial Micro-Strain Sensor Property and Sensing Principles

2.1. Configuration of ML-FMF

Figure 1 shows a cross section under microscope and measured index profile of the ML-FMF, which supports only the fundamental mode and LP_{11} mode groups.

By the cross section as shown in **Figure 1(a)**, the ML-FMF is consisted of a circular core area and a cladding layer. The bright part of the core area is a high refractive index layer which is achieved by doping the germanium. The dark part of the core area is a low refractive index layer which is achieved by doping fluoride, and the part outside the core area is the cladding, composed of pure silicon dioxide, whose refractive index is 1.444. **Figure 1(b)** shows the distribution of the refractive index of this fiber. The insets present the support modes simulated by the finite element method (FEM) in the presence of perfectly matched layer(PML) and scattering boundary conditions. The effective refractive indices of LP_{01} and LP_{11} groups are 1.44565 and 1.44605, respectively.

2.2. FM-FBG Properties and Sensing Principles

The excitation coefficients of LP_{01} and LP_{11} could be calculated by the overlap

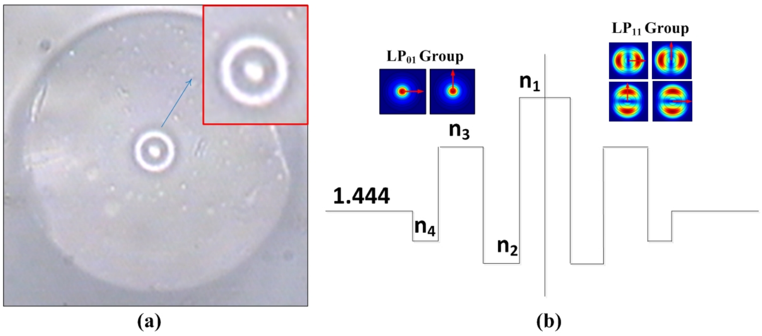

Figure 1. Characteristics of ML-FMF. (a) The micro-image of the cross-section; (b) Index profile and mode groups of the fiber.

integral between the Gaussian beam and the mode fields in **Figure 2(a)** according to Equation (1). The particularly designed ML-FMF supports only two mode groups with approximately equal excitation coefficients. And thus, the resulting FM-FBG has gain flattening spectral filter effect, which is beneficial to easy sensing detecting.

$$\eta_n = \frac{\iint_S \psi_S(x,y)\psi_n(x,y)dxdy}{\iint_S \psi_n(x,y)\psi_n(x,y)dxdy}. \quad (1)$$

$\psi_S(x,y)$, $\psi_n(x,y)$ and η_n are respectively the incident filed distribution, the guided mode distribution and excitation coefficient of the nth order mode in the FMF.

For simplicity, it is an assumption that the excited power of both guided modes is equal in the calculation. The theoretically calculated transmission and reflection spectral with conventional transfer matrix method is shown in **Figure 2(b)**. The self-coupling and cross-coupling will be considered between less contrapropagating modes, which would be gotten clear Bragg transmission resonances. The modes, LP_{01} and LP_{11} contra-propagating modes, couple to each other subjected to the mode phase matching condition given by Equation (2).

$$\lambda = (n_{eff,k}^{+} + n_{eff,j}^{-})\Lambda. \quad (2)$$

where $n_{eff,k}^{+}$, $n_{eff,j}^{-}$ and Λ are the effective refractive index of kth forward-propagating mode, the effective refractive index of jth backward-propagating mode and the grating period, respectively. The grating period using in this sensor probe is 537.5 nm and the grating length is determined by the uniform phase-mask.

The transmission spectrum of FM-FBG would be affected by environmental perturbation. This FM-FBG, as a sensing head, can sense it by the spectral dips drift. As the axial strain L increases, the fiber would be stretched to change length, which would make the Λ longer. The transmission spectrum could have a red-shifted.

3. Experimental and Discussion

The measured transmission spectrum is shown in **Figure 3**. As we can see on the

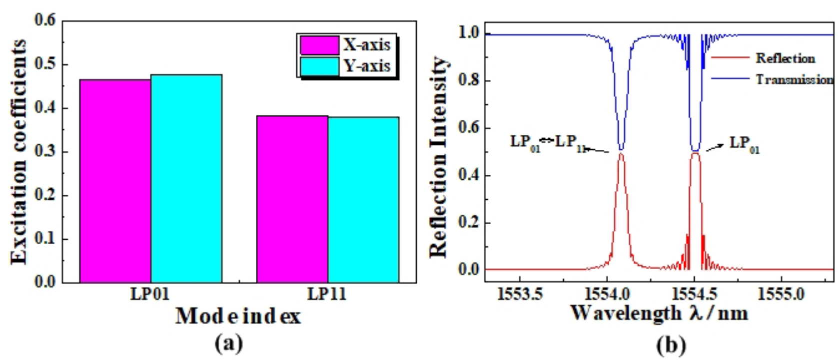

Figure 2. (a) Excitation coefficients for different modes; and (b) transmission and reflection spectra of the FM-FBG inscribed in the ML-FMF in calculation.

transmission spectrum, three dips correspond to the LP_{01} self-coupling, cross-coupling of two mode groups and LP_{11} self-coupling.

This experiment uses FM-FBG as a sensing head to measure the micro-strain along the fiber. **Figure 4** shows an axial micro-strain sensing experimental setup. The FM-FBG is secured by two fiber clips and straightened with a certain longitudinal stress. One is fixed and the other one can be elongated by the micro-adjuster, and the change of the axial micro-strain would be measured. The light of the broadband light source (KOHERASTM, superK uersa) is injected into the FM-FBG and the output spectrum is detected using a spectrometer (YOKOGAWATM, AQ6375) to observe the effect of strain on the transmission spectrum in real time.

For uniform strain, each micro-adjuster elongates the FM-FBG at a step of 208 με, and the range of 0 με - 1456 με is detected in this experiment. **Figure 5(a)** shows how the transmission spectrum drifts with the strain. It can be seen that the dips drift to long wavelengths. **Figure 5(b)** shows the relationship between

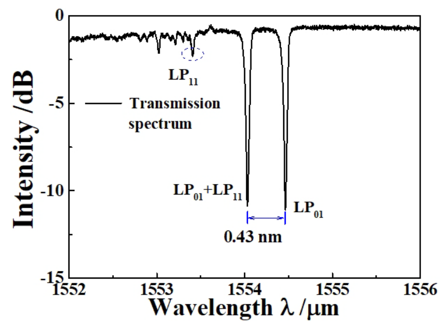

Figure 3. Schematic of the transmission spectrum in FM-FBG.

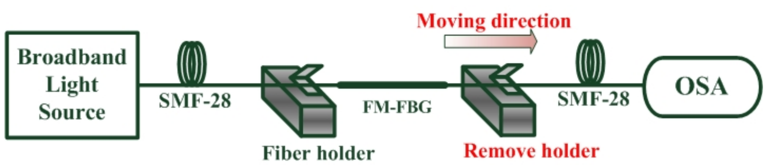

Figure 4. The experimental setup for axial micro-strain detection using the proposed FM-FBG.

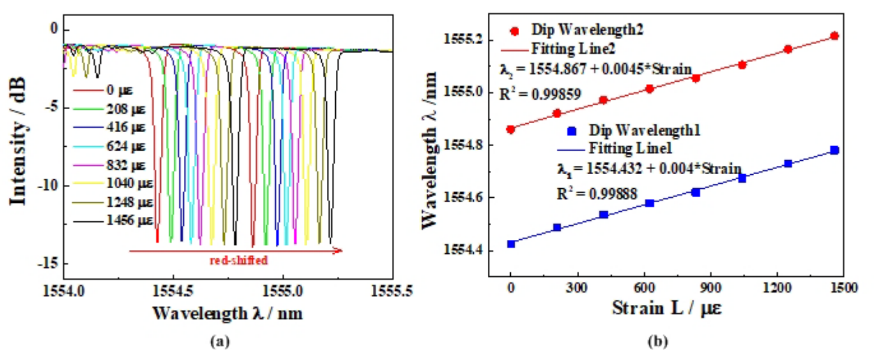

Figure 5. Experimental results: (a) Dips shift via the axial micro-strain changes; (b) The curve of the axial micro-strain vs. dips.

spectral resonance dips and strain changes. By fitting the experimental data, the fitting correlation coefficients R2 are respectively 0.99888 and 0.99859, which is indicating that the linear relationship of the sensing system is very accurate. The slopes of the fitted lines represent the axial strain sensitivity, with values of ~4 pm/με and ~4.5 pm/με, which are actually a little off. And it is caused by the different axial strain sensitivities of LP_{01} and LP_{11}. That may have a great potential for the simultaneous measurement of two parameters.

4. Conclusion

An in-fiber axial micro-strain sensor based on a FM-FBG inscribed in a novel dual-mode ML-FMF is demonstrated and experimentally characterized. The FM-FBG owned two resonant dips act as a sensing head, which would be one of the key techniques to achieve fiber grating distributed sensing network in internet of things. The axial strain sensitivity performs well. It is also simple, easy to manufacture, potentially low cost, and possesses a much larger measurement range.

Acknowledgements

This work was supported in part by the National Natural Science Foundation of China (61905293, 61774175, 61605003); Natural Science Foundation of Beijing Municipality (4181001); National Basic Research Program of China (2017YFB0405400); National Foundation Pre-research Academic Workshop of Minzu university of China (2020MDYY58).

Conflicts of Interest

The authors declare no conflicts of interest regarding the publication of this paper.

References

[1] Yin, G., *et al.* (2016) Determination of Optical Fiber Parameters Based on Fiber Gratings and a Search Procedure. *Journal of Lightwave Technology*, **35**, 3591-3596. https://doi.org/10.1109/JLT.2016.2626799

[2] Ghosh, C. and Priye, V. (2020) Highly Sensitive FBG Strain Sensor with Enhanced Measurement Range Based On Higher Order FWM. *IEEE Photonics Journal*, **12**, 1-7. https://doi.org/10.1109/JPHOT.2019.2912266

[3] Hu, H., *et al.* (2018) Investigation of Non-Uniform Gelation Effects on Residual Stresses of Thick Laminates Based on Tailed FBG Sensor. *Composite Structures*, **202**, 1361-1372. https://doi.org/10.1016/j.compstruct.2018.06.074

[4] Leal-Junior, A.G., *et al.* (2019) Simultaneous Measurement of Pressure and Temperature with a Single FBG Embedded in a Polymer Diaphragm. *Optics & Laser Technology*, **112**, 77-84. https://doi.org/10.1016/j.optlastec.2018.11.013

[5] Tong, R., *et al.* (2019) Simultaneous Measurement of RH and Temperature Based on FBG and Balloon-Like Sensing Structure with Inner Embedded Up-Tapered MZI. *Measurement*, **146**, 1-8. https://doi.org/10.1016/j.measurement.2019.06.018

[6] Sebastian, S., *et al.* (2019) Hydrostatic Pressure Response of Mo Coated Etched Fiber

Bragg Grating Sensor in Side-Hole Packaging. CLEO: Applications and Technology. Optical Society of America. https://doi.org/10.1364/CLEO_AT.2019.JTh2A.95

[7] Huang, J., *et al.* (2019) Effect of Hydrogen Gas on FBG-Based Optical Fiber Sensors for Downhole Pressure and Temperature Monitoring. *Optics Express*, **27**, 5487-5501. https://doi.org/10.1364/OE.27.005487

[8] Hung, H., *et al.* (2019) Apparatus and Method for Sensing Acceleration or Force Using Fiber Bragg Grating (FBG). Google Patents.

[9] Guo, J.-Y., *et al.* (2019) Simultaneous Measurement of Tilt Angle and Temperature Based on a Taper-Shaped Polymer Incorporating a Fiber Bragg Grating. 2018 *Conference on Lasers and Electro-Optics Pacific Rim* (*CLEO-PR*). *IEEE*. https://doi.org/10.1364/CLEOPR.2018.Th4L.4

[10] Zhao, Y., *et al.* (2018) Simultaneous Directional Curvature and Temperature Sensor Based on a tilted Few-Mode Fiber Bragg Grating. *Applied Optics*, **57**, 1671-1678. https://doi.org/10.1364/AO.57.001671

[11] Chen, X., *et al.* (2005) Optical Chemsensor Based on Etched Tilted Bragg Grating Structures in Multimode Fiber. *IEEE Photonics Technology Letter*s, **17**, 864-866. https://doi.org/10.1109/LPT.2004.842786

[12] Qiu, W., *et al.* (2013) Simultaneous Measurement of Temperature and Strain Using a Single Bragg Grating in a Few-Mode Polymer Optical Fiber. *Journal of Lightwave Technology*, **31**, 2419-2425. https://doi.org/10.1109/JLT.2013.2266791

[13] Yang, K., *et al.* (2017) Femtosecond Laser Inscription of Fiber Bragg Grating in Twin-Core Few-Mode Fiber for Directional Bend Sensing. *Journal of Lightwave Technology*, **35**, 4670-4676. https://doi.org/10.1109/JLT.2017.2750407

[14] Kim, H., *et al.* (2020) Microwave Curing Characteristics of CFRP Composite Depending on Thickness Variation Using FBG Temperature Sensors. *Materials*, **13**, 1720. https://doi.org/10.3390/ma13071720

[15] Li, L., *et al.* (2012) Novel NCF-FBG Interferometer for Simultaneous Measurement of Refractive Index and Temperature. *Photonics Technology Letters IEEE*, **24**, 2268-2271. https://doi.org/10.1109/LPT.2012.2226876